Journal of Applied Polymer Science

Experimental and Numerical Study of Distortion in Flat, L-shaped, and U-shaped Carbon Fiber–Epoxy Composite Parts

Pooneh Roozbehjavan, Behrouz Tavakol, Ashraf Ahmed, Hoda Koushyar, Rony Das, Ronald Joven, Bob Minaie

Department of Mechanical and Aerospace Engineering, California State University, Long Beach, California 90840
Correspondence to: B. Minaie (E-mail: Bob.Minaie@csulb.edu)

ABSTRACT: In this study, flat composite panels were fabricated to find the effect of different manufacturing parameters, including stacking sequence, part thickness, and tooling material, on distortion of carbon fiber-epoxy composite parts. L-shaped and U-shaped panels were also made to investigate the effect of stacking sequence on spring-in angle and warpage of the curved panels. Results showed that distortion of the flat panels caused by asymmetry in the stacking sequence was an order of magnitude greater than distortion of the panels with an unbalanced stacking sequence; whereas in the curved panels, the panel with an asymmetric stacking sequence showed the least spring-in angle, and the largest angle was observed in the symmetric panel. MSC Marc was used to predict distortion of the panels, and the simulation results were compared with the experimental results for several stacking sequences of the flat and the L-shaped panels. © 2014 Wiley Periodicals, Inc. J. Appl. Polym. Sci. **2014**, *131*, 40439.

KEYWORDS: composites; manufacturing; theory and modeling

Received 2 January 2013; accepted 15 January 2014
DOI: 10.1002/app.40439

INTRODUCTION

Residual stresses induced during curing of composite material parts could result in undesirable dimensional changes once the part is removed from the tool. Several factors could contribute to development of residual stresses during cure. The mismatch between the coefficient of thermal expansion (CTE) of resin and fiber,[1] and chemical shrinkage of the resin during cure[2–5] are considered as the most important sources of residual stress formation. Moreover, fiber misalignment, laminate defects such as voids, and tool-part CTE mismatch[3,6–8] could create residual stress during the manufacturing process of composite material parts.

Cured parts may exhibit different dimensional changes depending on the original geometry of the part. Warpage and spring-in are two common dimensional changes that occur during the cure of contoured-shape parts.[1,9–11] The unfavorable dimensional deviation of the cured parts leads to assembly process issues, which, in a worst case scenario, may result in rejection of the part.[12] The current industry practice is to determine final geometry of the cured part based on trial-and-error. An important part of the process is to modify the tooling geometry to compensate for the distortion of the cured part.[3] The current practice is time-consuming, costly, and imprecise. Prediction of curing distortion will help to overcome the current challenges facing the manufacturing of composite materials. Finite-element analysis (FEA) has been used to predict the distortion of contoured-shape composite parts.[13–15] However, laminate stacking sequence in most of these studies has been symmetric only.[1,13,14] Therefore, the effect of laminate asymmetry on the distortion of contoured-shape parts has not been studied extensively. As discussed in the present study, asymmetric stacking sequences reduce the spring-in angle in cured parts. In addition, while the current study demonstrates that 3D simulations are more sophisticated for an accurate estimation of distortion, many previously published studies have utilized simple 2D FEA to estimate the geometry of composite parts after curing.[15] It is also notable that only 3D models can accurately capture the warpage of the flat parts.[16]

This study presents an investigation into the effects of stacking sequence, thickness, and tooling material on distortion of composite parts. As stated before, previous studies have mostly investigated simple lay-up configurations such as balanced and symmetric laminates and have paid less attention to other stacking sequences. The effect of laminate balance and symmetry on the distortion of cured parts can be observed only when a variety of symmetric and asymmetric stacking sequences is studied. The results of such studies were used later to validate simulation results.

This study also presents a new approach to capturing 3D distortion patterns in panels with square geometry, based on scanning

Table I. Manufacturing Configuration of Flat, L-shaped and U-shaped Panels (Each Panel was Repeated Three Times)

Panel no.	Panel geometry	No. of plies	Panel stacking sequence	Panel type	Tooling material
1	Flat	16	$[0/45/90/-45]_4$	Asymmetric, balanced	Aluminum
2	Flat	16	$[0/45/90/-45]_{2S}$	Symmetric, balanced	Aluminum
3	Flat	16	$[0/45/90/45]_{2S}$	Symmetric, unbalanced	Aluminum
4	Flat	16	$[0/45/90/45]_4$	Asymmetric, unbalanced	Aluminum
5	Flat	8	$[0/45/90/-45]_S$	Symmetric, balanced	Aluminum
6	Flat	8	$[0/45/90/-45]_2$	Asymmetric, balanced	Aluminum
7	Flat	16	$[0/45/90/-45]_4$	Asymmetric, balanced	Steel
8	Flat	16	$[0/45/90/-45]_4$	Asymmetric, balanced	Composite
9	L-shape	16	$[0/45/90/-45]_4$	Asymmetric, balanced	Aluminum
10	L-shape	16	$[0/45/90/-45]_{2S}$	Symmetric, balanced	Aluminum
11	L-shape	16	$[0/45/90/45]_4$	Asymmetric, unbalanced	Aluminum
12	L-shape	16	$[0/45/90/45]_{2S}$	Symmetric, unbalanced	Aluminum
13	U-shape	16	$[0/45/90/-45]_4$	Asymmetric, balanced	Aluminum
14	U-shape	16	$[0/45/90/-45]_{2S}$	Symmetric, balanced	Aluminum

of both sides of the panels. Most previous studies have reported the 2D distortion of panels which were narrow on one side and sufficiently long on the other side only to eliminate the 3D nature of distortions.[17,18] However, the distortions that occur in cured panels are often 3D and the assumption of simple 2D distortions is far from the real case scenario. In addition, the proposed 3D scanning approach makes the comparison between simulation results and experimental observations easier and more accurate. Using this approach, distortion patterns can be obtained more accurately for complex geometries. Raghavan and Zeng reported the final 3D distortion pattern of the cured composite part by displaying discreet data points of a coordinate measurement machine CMM.[3] However, proposed method in this study provides more consistent data and, therefore, could be well utilized for comparison between experimental and simulation results which, in turn, could enhance the accuracy of simulations sufficiently to allow them to be used for industrial applications.

In this study, the effect of stacking sequence on the 3D distortion of L-shaped and U-shaped composite parts fabricated with IM7/977-2 UD was also investigated. A seven-axis Romer arm equipped with a laser scanner probe was utilized to scan the deformed cured parts. The scanning data was further analyzed with PolyWorks software to obtain the warpage and the spring-in angle. MSC Marc 2008r1 was utilized to conduct a during-cure 3D simulation of flat and L-shaped panels, and the obtained results were validated by the experimental data. In L-shaped panels, the effect of tool geometry and curve radius on the spring-in angle was also investigated. As will be shown later, the distortion of composite parts could be predicted more accurately with the 3D simulation.

TECHNICAL APPROACH

Experimental Study

Material and Process. In this study, IM7/977-2 UD (unidirectional) was used as the main material to fabricate the panels. This commercial unidirectional prepreg consists of IM7 carbon fibers impregnated with CYCOM 977-2, a curing toughened epoxy resin manufactured by Cytec Engineered Materials.[19] The resin's elastic modulus is 3.5 GPa and its tensile strength is 81 MPa. This epoxy resin is proposed for press molding and autoclave processing. IM7 is a continuous hex tow carbon fiber with tensile modulus of 276 GPa and tensile strength of 5,670 MPa. The high tensile strength and modulus along with good shear strength in IM7 fiber provide higher safety margins for applications with critical stiffness and strength. A fully cured IM7/977-2 UD prepreg shows elastic modulus of 165 GPa in longitudinal direction and about 9 GPa in through-thickness and transverse directions.

Flat panels, with a size of 430 × 430 mm^2, for the study of thickness and stacking sequence were cured on an aluminum tool with a size of 1800 × 700 mm^2 and a thickness of 12 mm. Composite and steel tools, both with a size of 600 × 600 mm^2 and a thickness of 12 mm were used to study the effect of tooling material on distortion. To fabricate L-shaped and U-shaped panels, a convex aluminum tooling was used with a geometry of 500 × 125 × 101 mm^3. Using the vacuum bagging method, all the thin panels were cured according to the manufacturer's recommended cure cycle. These panels were heated from room temperature up to 177°C with a rate of 2.78°C min^{-1}, were kept 3 h at this cure temperature (177°C), and finally, were cooled down to room temperature at a rate of 2.78°C min^{-1}. The maximum cure pressure of 586 kPa was applied during the cure cycle. A release agent (Frekote 770NC) was applied on the tool, and a release film (Airtech WL5200) was used in all cases to ease removal of the part from the tool and the caul plate. Using this release system, parts could easily be removed without applying a noticeable force once the vacuum bag was detached.

Panel Configuration. To study the effect of panel thickness, stacking sequence, and tooling material on the geometrical distortion, flat panels were fabricated using the eight manufacturing configurations listed in Table I. Thickness of the panels was

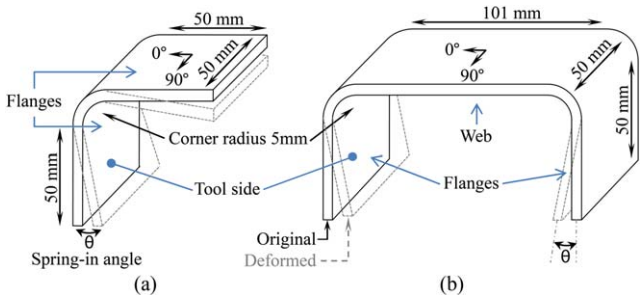

Figure 1. Schematic depiction of spring-in angle and geometry of (a) L-shaped, and (b) U-shaped panels. [Color figure can be viewed in the online issue, which is available at wileyonlinelibrary.com.]

kept under 32 plies in order to apply manufacturer's recommended cure cycle for a thin laminate. Note that each test was repeated three times. Additionally, the size of the panels and the number of plies (thickness) were chosen based on the dimensions of those used by previous researchers.[16]

U-shaped and L-shaped panels (see Figure 1) were also fabricated to investigate the effect of part shape on the residual stresses and geometrical distortion induced during the curing process. These panels were laid-up on a convex aluminum tool using the stacking sequences described in Table I. As shown in this table, several stacking sequences were considered in fabrication of the panels to study the effect of fiber orientation on the processing-induced geometrical distortion. Sixteen layers were used for all the samples, resulted in a thickness of about 2 mm.

Measuring Method for Flat Panels. A seven-axis Romer arm equipped with a laser scanner probe with a minimum point-to-point resolution of 42 μm was utilized to obtain 3D pattern of distortion and maximum amount of distortion for each panel. Measuring the maximum distortion, a surface was created using the scanned data and three corners of the surface were fixed on a flat reference surface. The maximum distortion was defined as the maximum distance between the positioned surface and the reference surface. The 3D pattern of distortion was also established for each panel by comparing each point of the positioned surface with an equivalent point on the reference surface using PolyWorks. The panels were held vertically during the scan to minimize effect of weight on the measured distortion.

Measuring Method for L-shaped and U-shaped Panels. Distortion of the L-shaped and the U-shaped panels was categorized into two parts: warpage and spring-in angle. As illustrated in Figure 1, spring-in angle was defined as the angle formed between the deformed shape and the original shape of the panel. In addition, warpage was observed in the flanges of the L-shaped panels and the webs and the flanges of the U-shaped panels as a deviation in flatness from their original shape.

The seven-axis Romer was also used to scan the tool side and the bag side of the panels. The spring-in angle was obtained for the tool-side of the panels with different stacking sequences by analyzing the data in PolyWorks. The 3D warpage pattern was also achieved for the flat sections of the panels. Similar to the flat panels, a surface was created from the scanned data obtained from the flat sections of the panel and subsequently compared to a flat reference surface to obtain the warpage pattern.

Numerical Study

MSC Marc 2008r1 was utilized to conduct 3D simulations aimed at estimating the distortion of L-shaped and Flat carbon fiber-epoxy composite panels. For this purpose, distortion was modeled using virtual panels with the dimensions mentioned in Table I. Subsequently, simulation results were compared with the experimental data obtained by the abovementioned 3D scanning. The simulation methodology was introduced in a previous study of authors for flat panels.[16] As shown in the study, several Fortran codes were incorporated into the model to account for different phenomena including cure shrinkage,[20] cure kinetics, thermal strains,[21] tool-part interaction,[22] and development of mechanical properties during cure. Different models were also implemented into the simulation to estimate development of the material properties during cure. For instance, Springer–Loos[23] model was used to estimate the degree of cure, and a modified version of Bogetti–Gillespie[24] model was utilized to account for the effect of cure shrinkage on distortion of the composite part.

In this study, the former computational model was extended to flat panels with different stacking sequences and other geometries such as L-shaped panels and the results were compared with the experimental results.

Flat Panel. The 3D simulations were conducted for flat panels to estimate the maximum value of distortion as well as the 3D distortion pattern. As shown in previous work of the authors[16] each composite panel was confined by the caul plate on the top and the tool at the bottom. To mimic autoclave conditions, a temperature cycle was applied on free surfaces of the tool and the caul plate, and pressure cycle was exerted on the caul plate to indirectly consolidate the panel. Notice that an eight-node composite brick element was used, which comprised of different layers with individually defined thickness, material properties, and orientation.

L-shaped Panel. A methodology similar to that used for flat panel was implemented to estimate the warpage and spring-in angle of L-shaped panels using a 3D model. Figure 2 illustrates the finite element mesh used for the panel and the tool. A temperature cycle was applied on free surfaces of the tool and top of the panels, whereas autoclave pressure was applied only on top of the part. The asymmetric stacking sequences were considered intentionally to show capability of the simulation in an estimation of more complicated cases. To study the effect of curve radius on the spring-in angle of L-shaped panels, two panels with curve radii of 23 and 5 mm were simulated. In addition, to investigate the effect of tool geometry on spring-in angle, curing of an L-shaped panel with a curve radius of 5 mm was simulated on tools with two different geometries (concave and convex).

RESULTS AND DISCUSSION

Flat Panels

Effect of different stacking sequences, part thickness, and tooling material on distortion of composite parts was investigated

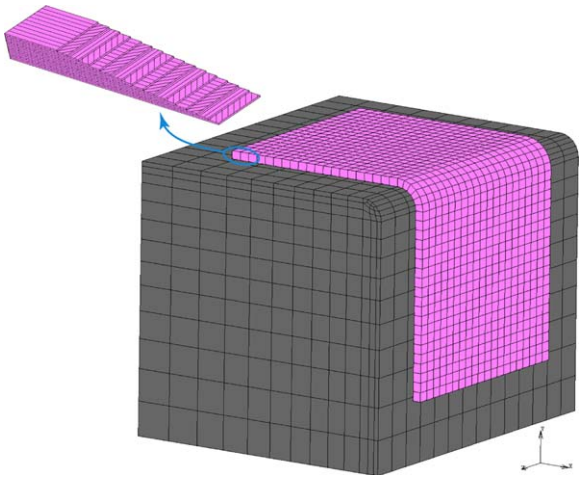

Figure 2. The 3D finite element mesh used for the L-shaped panel cured on an aluminum tool. [Color figure can be viewed in the online issue, which is available at wileyonlinelibrary.com.]

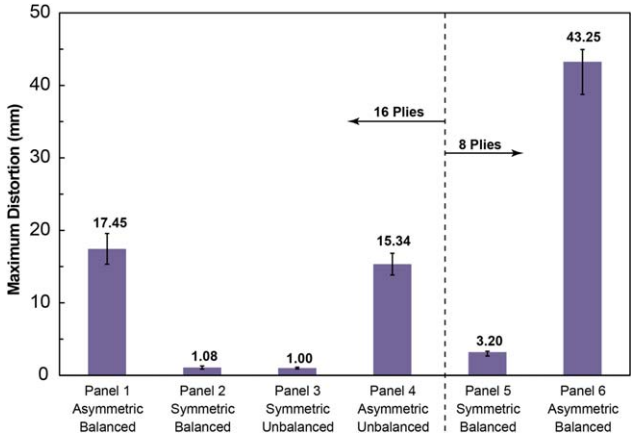

Figure 3. Maximum distortion in tool side of Panel 1 to Panel 6 (effect of stacking sequence and thickness). [Color figure can be viewed in the online issue, which is available at wileyonlinelibrary.com.]

using a 3D FEA computational approach, and results were compared with distortion measured in real parts.

Stacking Sequence. To determine the effect of stacking sequence on distortion of the flat panels, 3D distortion patterns were obtained for panels 1 to 4 (Table I). For this purpose, the maximum distortion was measured using the CMM scanner described in Experimental Study section, and results were portrayed in Figure 3. As indicated in this figure, the maximum amount of distortion was strongly influenced by the stacking sequence since the results showed higher geometrical distortion in asymmetric panels when compared with the symmetric ones. Note that the variance in the maximum amount of distortion between panel 2 and 3 could be attributed to inherent error of the experimental methodology. Therefore, it could be assumed that the maximum distortion of the symmetric panels (2 and 3), once the panel thickness was increased, did not depend on the state of being balanced or unbalanced. On the other hand, once the panel was asymmetric, unbalanced stacking sequences could decrease the maximum distortion and compensate the effect of asymmetry.

Part Thickness. Effect of part thickness on geometrical distortion was quantified by comparing the distortion obtained from panels 1, 2, 5, and 6 (see Table I), and results were shown in Figure 3. Note that panels 2 and 5 were laid-up using a symmetric and balanced stacking sequence ($[0/45/90/-45]_{nS}$), but the amount of plies was different since panel 2 was twice as thick as panel 5. Furthermore, the distortion measured in panel 1 was compared with that of panel 6 to find the effect of thickness on distortion of asymmetric and balanced panels. The results indicated that, in agreement with the previous section, asymmetric panels depicted a higher amount of geometrical distortion than symmetric ones. Furthermore, it was evident that the thinner panel showed larger distortion due to reduced stiffness of the panel. These results show satisfactory agreement with previous studies.[17,18]

Tooling Material. To investigate the effect of tooling material on distortion of a composite part, three panels were fabricated using three different tools (aluminum, steel, and carbon fiber-epoxy composite) while the other conditions were kept the same. The stacking sequence of an asymmetric/balanced panel $[0/45/90/-45]_4$ was taken into account since the abovementioned findings indicated that this stacking sequence resulted in a large amount of distortion compared with other stacking sequences. The 3D pattern of distortion on the tool-side of the panels cured on steel (panel 7) and composite tools (panel 8) were compared with the distortion of the tool-side in panel 1, which was cured on aluminum.

Using different tools resulted in different amount of distortion in the panels because the tool-part interaction induced various amount of residual stresses particularly due to thermal expansion mismatch between the tools and the panels.[22] As shown in Table II, panel 1 (cured on the aluminum tool) represented greatest amount of distortion among the three panels while panel 8 (cured on the composite tool) had the minimum distortion, although the difference in the distortion between these panels was 7%. Therefore, tool-part interface had a low contribution to developing residual stresses, which agreed with the literature where it was stated that tooling conditions do not have a significant effect on distortion of composite parts with flat geometry.[13]

Finally, results of 3D scanning indicated similar distortion patterns for the three panels (1, 7, and 8), which was attributed to the fact that they were fabricated with the same stacking sequences.

Table II. Effect of Tool–Part Interface on Distortion of the Composite Part

	Tooling material		
	Aluminum	Steel	Composite
Maximum distortion (mm)	17.45 ± 2.12	17.28 ± 2.23	16.1 ± 1.02

Comparison of Experimental Results with Simulation Results for Flat Panels

Simulation of distortion was conducted for panels with different stacking sequences and thicknesses (panels 1–6 of Table I). The simulation results were compared with those obtained experimentally, and results were shown in Figure 4. From these results, the maximum amount of distortion was obtained for all the fabricated and simulated flat panels (see Table III). To assess for the accuracy of the computational model, a statistical treatment was performed for comparison of the experimental results with the simulations by using a T-test with α equal to 0.05. This T-test resulted in a P value of 0.77, which is greater than α, thus indicating that the difference between the experimental results and the simulations is not statistically significant. In summary, simulations showed a satisfactory agreement with experimental results for the maximum amount of distortion.

The model accurately predicted the maximum amount of distortion in most of the panels, except in panel 4 where an error up to 30% was measured. This error was attributed to the fact that an asymmetric and unbalanced stacking sequence encounters several load couplings that may not be estimated accurately by the numerical analysis performed in this research. Therefore, the analysis of this complex state of stress is proposed as a future area of research to improve the numerical analysis and to develop appropriate models for this particular case of asymmetric and unbalanced stacking sequences. Furthermore, modules corresponding to the behavior of stress relaxation[25] and resin flow[26] should be incorporated into the FEA model.

Additionally, Figure 4 portrays comparison between the simulated and the experimental 3D distortion patterns for the panels. Results indicated that the model could predict the distortion pattern in all the measured panels since the simulation successfully predicted the experimental pattern for panels 1, 2, and 4. Although panel 3 [Figure 4(c)] showed a large discrepancy, note that the distortion pattern was predicted from the top right corner toward the bottom left corner as obtained experimentally.

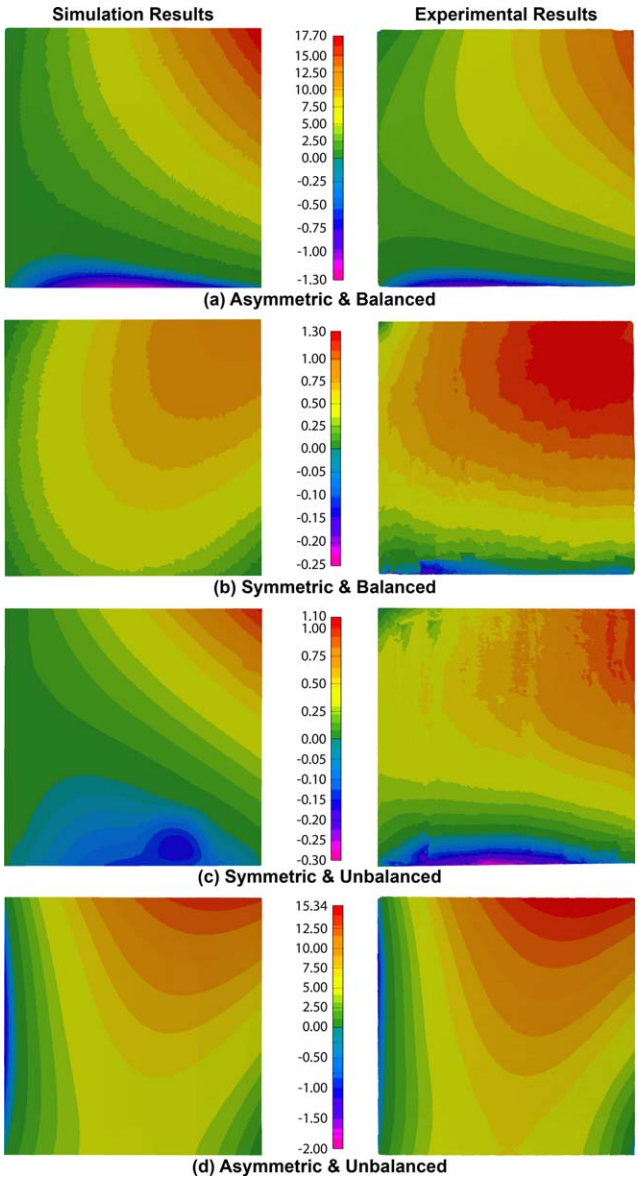

Figure 4. Comparison of tool-side distortion pattern for (a) Panel 1, (b) Panel 2, (c) Panel 3, and (d) Panel 4. [Color figure can be viewed in the online issue, which is available at wileyonlinelibrary.com.]

L-shaped and U-shaped Panels

Stacking Sequence. Figure 5 shows spring-in angle in the L-shaped panels with various stacking sequences. As shown in the

Table III. Comparison of Simulation Results with Experimental Results for Maximum Distortion of Flat Panels with Various Stacking Sequences and Different Thicknesses

			Maximum amount of distortion (mm)	
Panel no.	No. of plies	Panel type	Experiment	Simulation
1	16	Asymmetric, balanced	17.45 ± 2.12	17.70
2	16	Symmetric, balanced	1.08 ± 0.22	1.02
3	16	Symmetric, unbalanced	1.00 ± 0.12	1.02
4	16	Asymmetric, unbalanced	15.34 ± 1.5	13.46
5	8	Symmetric, balanced	3.20 ± 0.53	3.15
6	8	Asymmetric, balanced	43.25 ± 4.5	30.23

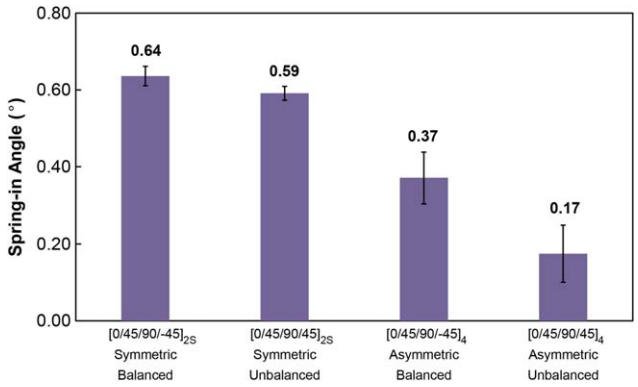

Figure 5. Effect of stacking sequence on spring-in angle of the L-shaped panels. [Color figure can be viewed in the online issue, which is available at wileyonlinelibrary.com.]

figure, the panel having a symmetric and balanced stacking sequence showed the largest spring-in angle, while the panel with asymmetric and unbalanced stacking sequence had the least spring-in angle. In addition, higher warpage was obtained in the flanges of the asymmetric panels compared with the symmetric panels (see Figure 6). Warpage of the flanges could be one reason to make less spring-in angle in the panels with the asymmetric stacking sequences.

The effect of symmetry on the spring-in angle of the U-shaped panels was also investigated. Table IV shows the spring-in angles in the U-shaped panels compared to the spring-in angles of the L-shaped panels with the identical stacking sequences. In general, the U-shaped panels resulted in larger spring-in angles than the L-shaped panels, as shown in previous studies,[1] because of more geometry locking once the part was removed from the tool.

The effect of symmetry on warpage in U-shaped and L-shaped panels was also investigated. For this purpose, same flanges of two panels with asymmetric and symmetric stacking sequences were selected. As illustrated in Figure 6(a,b), the asymmetric panels showed higher warpage compared with the symmetric panels. Similar results were obtained in flat panels with symmetric and asymmetric stacking sequences. A maximum distortion of 0.84 mm was observed for the U-shaped panel with the balanced and asymmetric stacking sequence, while the balanced and symmetric U-shaped panel had 0.33 mm for maximum distortion. Comparing color bar in Figure 6(a) with the one in Figure 6(b) shows that the U-shaped panels resulted in more than twice as much warpage as the L-shaped panels. Patterns of warpage are shown for webs of the U-shaped panels having two different stacking sequences of symmetric and asymmetric [Figure 6(c)]. Likewise as with other cases, the asymmetric panel was distorted more than the symmetric one.

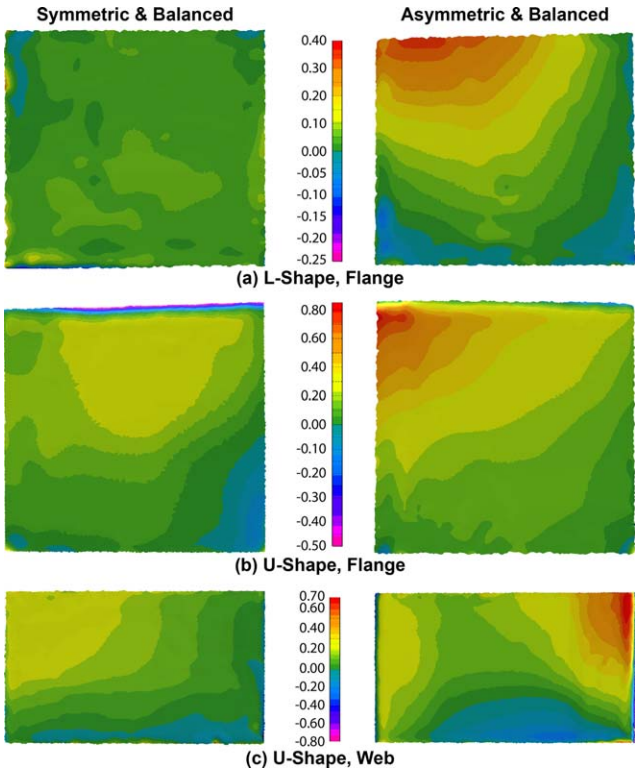

Figure 6. The 3D warpage patterns in (a) flanges of the L-shaped panels, (b) flanges of the U-shaped panels, and (c) webs of the U-shaped panels. [Color figure can be viewed in the online issue, which is available at wileyonlinelibrary.com.]

Comparison of Experimental Results with Simulation Results for L-shaped Panels

Effect of Stacking Sequence. Effect of stacking sequence on dimensional changes of the L-shaped and the U-shaped parts during the curing process has been discussed in detail in Stacking Sequence section. In this section, the curing process of the L-shaped panels with asymmetric stacking sequences was simulated as explained previously to predict the dimensional changes during cure. As shown in distortion of flat panels (Stacking Sequence section), the asymmetric stacking sequences resulted in more residual stresses and consequently more distortion compared to the symmetric stacking sequences. Therefore, in this section, asymmetric stacking sequences were considered for simulation of L-shaped parts because they represent the worst-case scenario for distortion due to residual stresses. Figure 7 depicts the comparison of simulation results with the

Table IV. Comparison of the Experimental Results for Spring-in Angle in U-shaped and L-shaped Panels

			Spring-in angle (°)	
Panel stacking sequence	No. of plies	Panel type	L-shaped	U-shaped
$[0/45/90/-45]_{2S}$	16	Symmetric, balanced	0.64	1.48
$[0/45/90/-45]_4$	16	Asymmetric, balanced	0.37	0.88

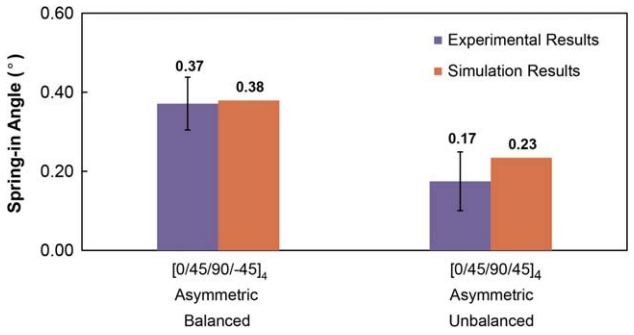

Figure 7. Comparison of simulation and experimental results for the L-shaped panels with asymmetric-balanced and asymmetric-unbalanced stacking sequences. [Color figure can be viewed in the online issue, which is available at wileyonlinelibrary.com.]

experimental results for both balanced and unbalanced panels. Satisfactory agreement was obtained between the simulation results and the experimental results; therefore, asymmetric and balanced stacking sequence was chosen for further investigation to predict the effect of curve radius and tool geometry on spring-in angle of an L-shaped part presented in following sections.

Effect of Curve Radius. Simulation was conducted for the stacking sequence of $[0/45/90/-45]_4$ to study the effect of curve radius on the spring-in angle. Simulation results showed that an L-shaped panel with a larger curve radius resulted in bigger spring-in angle [Figure 8(a,b)]. Larger curvature would result in greater residual stress due to higher geometry locking or more composite material involved in the curvature section which would cause the spring-in angle. Significant warpage was obtained in both panels due to asymmetry of the stacking sequences.

Effect of Tool Geometry. Finite element analysis was conducted to investigate the effect of tooling geometry on the spring-in angle of an L-shaped panel. For the stacking sequence of $[0/45/90/-45]_4$, the L-shaped panel cured on a concave tool resulted in 30% less spring-in angle compared with the identical panel cured on a convex tool [Figure 8(c,b)] in agreement with Radford's study.[27]

Distortion in composite parts is a costly and time-consuming issue in industry. The authors are introducing a methodology to address the problem and reduce the cost/time. As proposed, less geometry locking occurs using a concave tool compared to the panel cured on a convex tool, resulting in less spring-in angle, although it may involve a one-time cost increase for the tool.

CONCLUSIONS

In this study, a methodology was presented and a Romer arm, equipped with a laser scanning probe along with Polyworks software were used to obtain a 3D distortion pattern for composite panels. Using current method, not only was a 3D continuous distortion pattern obtained, but also the location and amount of maximum distortion was determined for each panel.

Effect of stacking sequence and panel thickness on distortion of the flat parts was investigated. The results revealed that distortion primarily depends on symmetry in the stacking sequence and not balance. For the panels with similar types of stacking sequences but different thicknesses, it was found that the eight-ply panels were distorted more than twice as much as the sixteen-ply panels. Study of different tooling materials revealed that maximum distortion is aggravated by increasing the CTE mismatch between the part and the tool; however, the difference between maximum amounts of distortion in such panels was <7% especially due to lack of geometry locking in flat parts.

A similar study was performed on L-shaped and U-shaped parts to find out effect of stacking sequence on warpage and spring-in angle of the panels. Among all of the L-shaped panels, the one with unbalanced and asymmetric stacking sequence showed the least spring-in angle, and the balanced and symmetric panel had the most spring-in angle. Although asymmetric panels had less spring-in angle compared to the symmetric ones, greater warpage was observed in the flanges of the panels with asymmetric stacking sequences. Similar results were also obtained for the U-shaped panels. However, the U-shaped panels generally showed greater spring-in angle than the L-shaped panels.

MSC Marc was utilized to simulate distortion of the panels. The simulation results for flat and L-shaped parts with different stacking sequences were validated by the experimental results. Using simulation, effect of tool geometry and curve radius on

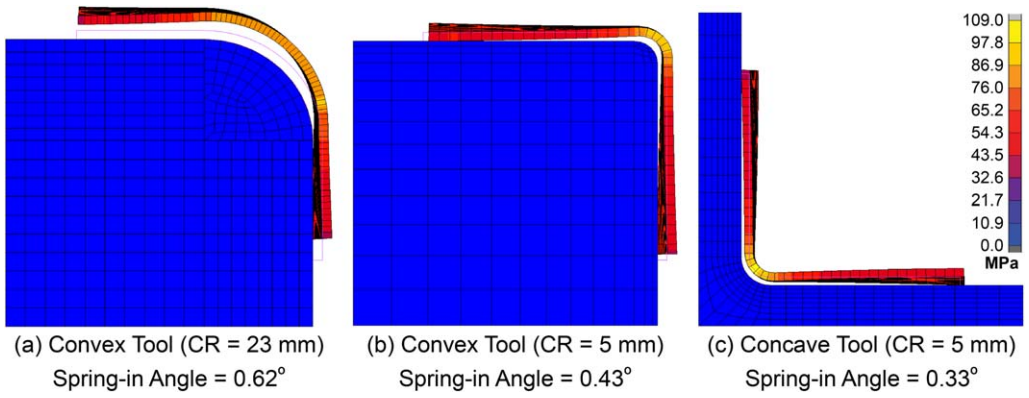

Figure 8. Effect of curve radius and tool geometry on spring-in angle of the L-shaped panel (scale factor of 3 is used for illustration purposes). [Color figure can be viewed in the online issue, which is available at wileyonlinelibrary.com.]

the spring-in angle of an L-shaped panel was studied. It was observed that the L-shaped panel with larger curve radius showed a greater spring-in angle. It was also shown that the spring-in angle in the L-shaped panel laid on a concave tool was 30% less than that for the identical panel cured on a convex tool.

REFERENCES

1. Albert, C.; Fernlund, G. *Compos. Sci. Technol.* **2002**, *62*, 1895.
2. Rennick, T. S.; Radford, D. W. In proceedings of the 28th International SAMPE Technical Conference, Seattle, WA, USA, Nov 4–7, **1996**.
3. Zeng, X.; Raghavan, J. *Compos. A Appl. Sci. Manufact.* **2010**, *41*, 1174.
4. Shah, D. U.; Schubel, P. J. *Polym. Test.* **2010**, *29*, 629.
5. Schubel, P. J.; Warrior, N. A.; Rudd, C. D. *Plast Rubber Compos* **2007**, *36*, 428.
6. Pagliuso, S. Progress in Science and Engineering of Composites, In proceedings of the 4th International Conference on Composite Materials; Tokyo, Japan, **1982**; p 1617.
7. Wisnom, M. R.; Ersoy, N.; Potter, K.; Clegg, M. *J. Compos. A* **2005**, *36*, 1536.
8. Ridgard, C. SME; Dearborn: MI, **1993**; p 1.
9. Arafath, A. R. A.; Vaziri, R.; Poursartip, A. *Compos. A Appl. Sci. Manufact.* **2009**, *40*, 1545.
10. Causse, E. R. P.; Trochu, F. *Compos. A Appl. Sci. Manufact.* **2012**, *43*, 1901.
11. Salomi, A.; Garstka, T.; Potter, K.; Grecoand, A.; Maffezzoli, A. *Compos. Sci. Technol.* **2008**, *68*, 3047.
12. Wisnom, M. R.; Potterand, K. D.; Ersoy, N. *J. Compos. Mater.*, **2007**, *41*, 1311.
13. Fernlund, G.; Rahman, N.; Courdji, R.; Bresslauer, M.; Poursartip, A.; Willden, K.; Nelson, K. *Compos. A Appl. Sci. Manufact.* **2002**, *33*, 341.
14. Dong, C. *J. Compos. Mater.* **2009**, *43*, 2639.
15. Kim, B.-S.; Bernet, N.; Sunderland, P.; Manson, J.-A. *J. Compos. Mater.* **2002**, *36*, 2389.
16. Tavakol, B.; Roozbehjavan, P.; Ahmed, A.; Das, R.; Joven, R.; Koushyar, H.; Rodriguez, A.; Minaie, B. *J. Appl. Polym. Sci.* **2012**, *128*, 941.
17. Radford, D. W. *J. Reinforc. Plast. Compos.* **2010**, *29*, 1875.
18. Twigg, G.; Poursartip, A.; Fernlund, G. *Compos. A Appl. Sci. Manufact.* **2004**, *35*, 121.
19. Cytec Eng. Materials, Cycom 977-2 Datasheet. Available at: http://cytec.com/engineered-materials/products/Datasheets/CYCOM%20977-2.pdf (accessed September 12 2012).
20. Das, R.; Tavakol, B.; Ahmed, A.; Minaie, B. In proceedings of the 56th International SAMPE Conference, Long Beach, CA, USA, May 23–26, **2011**.
21. Pardini, L. C.; Gregori, M. L. *J. Aerospace Technol. Manage.* **2010**, *2*, 183.
22. Joven, R.; Tavakol, B.; Rodriguez, A.; Guzman, M.; Minaie, B. *J. Appl. Polym. Sci.* **2013**, *129*, 2017.
23. Loos, A. C.; Springer, G. S. *J. Compos. Mater.* **1983**, *17*, 135.
24. Bogetti, T. A.; Gillespie, J. W., Jr. *J. Compos. Mater.* **1992**, *26*, 626.
25. Das, R.; Roozbehjavan, P.; Joven, R.; Ahmed, A.; Minaie, B. In Proceedings of the 44th International SAMPE Technical Conference, Charleston, SC, USA, OCT 22–25, **2012**.
26. Hubert, P. *Aspects of Flow and Compaction of Laminated Composite Shapes During Cure*, Ph.D. Thesis, The University of British Columbia, Vancouver, BC, Canada, July, **1996**.
27. Radford, D. W. *Compos. Eng.* **1995**, *5*, 923.